

Photorefractive effect due to a photoinduced surface-charge modulation in undoped liquid crystals

P. Pagliusi and G. Cipparrone*

Dipartimento di Fisica, LiCryL-Liquid Crystals Laboratory and INFM, Università della Calabria, I-87036, Rende (CS), Italy

(Received 27 November 2003; published 4 June 2004)

We demonstrate that some peculiarities of the surface-induced photorefractive effect (SIPRE) in undoped nematic planar cells can be simply explained considering the electric field induced by a modulated surface-charge distribution. Polarization-dependent forced light scattering and two-beam coupling experiments indicate that the observed anisotropy of the diffraction efficiency and the energy transfer between the pump beams strongly depend on the experimental geometry. The investigation suggests that the unusual dichotomy between local and nonlocal behavior can be ascribed to a modulated longitudinal electric field component, in phase with the interference pattern, which is not accountable by the conventional photorefractivity. In a simple and general approach we demonstrate that the conceived charge distribution model for the SIPRE produces a space-charge field having two orthogonal modulated components, in-phase and $\pi/2$ out of phase, respectively. The electric field configuration within the nematic sample gives reason for the main experimental features.

DOI: 10.1103/PhysRevE.69.061708

PACS number(s): 42.70.Df, 42.65.Hw, 73.30.+y, 41.20.Cv

I. INTRODUCTION

In recent years, photorefractive (PR) materials have been extensively studied and several applications in holographic interferometry, optical processing, and high-density data storage have been proposed because of their unique nonlinear optical properties [1–4]. Observation and investigation of photorefractivity in organic materials such as doped organic crystals and polymers [5,6] extended this research field, previously restricted to inorganic substances, increasing the feasible involved processes [3,4,7–12]. The PR effect is generally due to a combination of various physical mechanism such as photoinduced charge generation, charge carrier transport, and the electro-optic effect. It consists in a spatial modulation of the refractive index due to a charge redistribution in electro-optical materials, which takes place when they are inhomogeneously illuminated. Photoinduced generation and transport of charge carriers occur as a consequence of modulated light intensity, thus producing a non-uniform space-charge configuration. Due to the material's electro-optical response, the spatially modulated internal electric field, usually phase shifted with respect to the intensity pattern, modifies the refractive index creating a phase grating [2].

The PR effect in liquid crystalline materials has been investigated in different systems such as dye-, fullerene-, and carbon-nanotube-doped liquid crystals (LCs) [4,7,11,13], under the simultaneous application of light pattern and dc electric field, where huge optical nonlinearities have been achieved for low laser intensity [11]. The opportunity to create highly sensitive optical devices makes PR LC systems attractive for applications. In these cases, in fact, the orientational PR effect plays a fundamental role because of the large LC dielectric anisotropy and birefringence, which lead to a strong field dependent molecular reorientation. Orienta-

tional PR gratings have been also investigated in polymer dispersed liquid crystals (PDLCs) [9,14] and in LC film sandwiched between photoconductive polymeric layers [8].

Recently, a surface-charge induced PR effect (SIPRE) has been reported in undoped nematic liquid crystal (NLC) cells, where nonphotoconductive polymer has been used as aligning layer [12,15]. The fundamental role of the LC-polymer interface has been suggested by the investigation on four different kinds of planar NLC cells made with different non-photoconductive polymers and different NLCs [12]. Two-beam coupling (TBC) analysis in proper experimental geometry supported the occurrence of an orientational PR grating, $\pi/2$ phase shifted with respect to the interference pattern. Nevertheless, some details were appreciably different from the conventional PR effect in similar materials: the absence of a photocharge generator inside the LC, the nonphotoconductive polymers as aligning substrates, and the evidence of a complementary role of the two components of the interface according to which a sort of chemical and/or physical affinity is needed to observe grating formation [12]. An ample characterization of the PR-like orientational gratings has been performed for PTP-502 (tolane derivative from Merck KGaA, Darmstadt) cells aligned with rubbed polyimide [16], and for E7 (eutectic mixture of cyano-biphenyls and cyanoterphenyls) cells aligned with rubbed polyvinyl alcohol (PVA) substrates [17]. Photoinduced electric current and birefringence investigations [18,19], performed under uniform irradiation, confirmed the redistribution of charges at the interface and the consequent director reorientation in the NLC cell. The birefringence measurements reported in Ref. [19] proved that, in the low dc voltage regime, the voltage mainly drops on the thin electric double layers at the interfaces as a consequence of the dark charge carriers, collected to the border surfaces by the external dc field. Uniform irradiation with proper wavelength reduces the interfacial charge density, through an asymmetric photoelectric interface activation (PIA) [18], and induces molecular reorientation in the LC due to a rearrangement of the electric field [19]. Different

*Electronic address: cipparrone@fis.unical.it

proposed mechanisms, as light-induced desorption of charges and modulation of the anchoring conditions [15,20], have been discussed and ruled out [18,19].

The reported results and remarks suggested a kind of PR effect, a surface-induced photorefractive effect (SIPRE), in which no photogeneration of charges occurs in the LC bulk or in the aligning layers; but the irradiation modulates the charge distribution near the LC-polymer interface, through charge carriers photoinduced injection and recombination [18]. The resulting electric field in the LC bulk induces the reorientation of the nematic director through the dielectric effect, as for standard photorefractivity in LCs [4,11].

In this article, we demonstrate that the strongly anisotropic gratings in a NLC cell due to the SIPRE can be simply explained considering the electric field produced by a modulated charge distribution at the surface. The main goal of the proposed approach is that the nonlinear optical effect can be local or nonlocal with respect to the interference pattern depending on the experimental geometry [21]. Forced light scattering (FLS) and TBC measurements have been performed in undoped PVA-E7 planar cells for two different orientations between the cell optical axis and the grating vector. The FLS experiments reveal a strong anisotropy of the diffraction efficiency that reverses its sign changing the geometry. The TBC experiments prove that the energy coupling is strongly determined by the cell optical axis and the grating vector relative orientation. When they are parallel significant energy transfer between the transmitted pump beams is observed. On the contrary, when the cell optical axis and the grating vector are perpendicular no gain is detected. The TBC characterization by means of the grating translation technique demonstrates a refractive index grating which is $\pi/2$ phase shifted with respect to the interference fringes in the first geometry, and an in-phase grating in the second geometry, whereas the refractive index modulation amplitudes Δn are similar. In the following, we discuss a simple space-charge distribution model for the SIPRE, recently proposed in Ref. [21], which is able to account for both the local and nonlocal nonlinear optical response, observed in the investigated geometries. This model, even very simple, gives details of the main feature that distinguishes the orientational PR effect induced by a modulated surface-charge distribution (SIPRE), from the conventional PR effect related to photo-generated charge modulation in the bulk. The resulting space-charge field in the cell, which is here calculated neglecting the intrinsic LC's dielectric anisotropy [22], is proved to have two orthogonal modulated components: a $\pi/2$ phase-shifted component along the grating vector and an in-phase longitudinal component. Through the dielectric response of the NLC, the actual electric field configuration gives an explanation for the peculiar features of the SIPRE. It is worth to point up that the simple reported approach can be easily extended to calculate the electric field in other experimental configurations, such as LCs sandwiched between thin photoconductive layers [8].

II. EXPERIMENTS AND RESULTS

The experiments have been carried out on 30- μm -thick planar cells filled with the eutectic LC mixture E7 (BL001

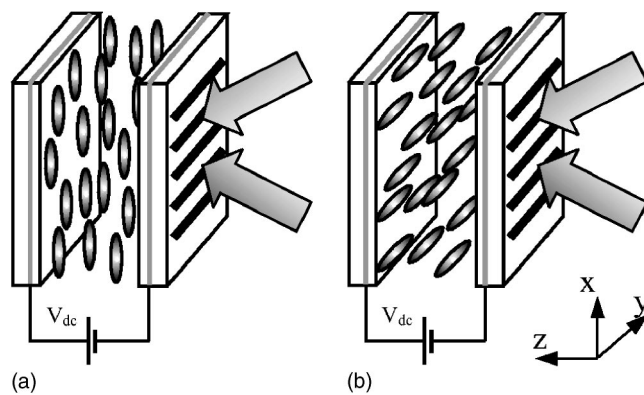


FIG. 1. Experimental configurations for wave-mixing investigations. The cell optical axis is parallel (a) or perpendicular (b) to the grating vector.

from Merck, Ltd., England). A thin polymer film (≈ 10 nm) was layered by spin coating of a PVA (87–89% hydrolyzed, molecular weight 31 000–50 000, from Aldrich) aqueous solution (0.5% by weight) on indium tin oxide (ITO) coated glass slides. After baking at 120°C for an hour and slow cooling to room temperature, the PVA film was gently rubbed with a velvet cloth in order to obtain uniform planar NLC alignment, with small pretilt angle ($\theta_0 \sim 10^{-2}$ rad). The cell was assembled by putting 30- μm -thick Mylar spacers between two parallel-oriented PVA-coated glasses and gluing them together with epoxy resin, then is filled with the LC mixture in nematic phase at room temperature.

The first investigations on the diffraction grating features have been performed by means of a usual pump-probe technique for FLS analysis [16]. Two coherent Ar^+ -ion laser beams ($\lambda = 457.9$ nm) of equal intensities I_0 , lie on the xz plane (plane of incidence) and cross on the sample in a non-tilted geometry, i.e., the bisector of the angle between the pump-beams is normal to the cell surface, while a dc voltage ($V_{dc} = 3$ V) is applied to the ITO electrodes. The pump beams are both linearly polarized in the plane of incidence (p) or perpendicular to it (s), in order to obtain a pure intensity modulation, whose spatial periodicity is $\Lambda \approx 40$ μm (Raman-Nath regime). Two geometries have been investigated. In the first one, both pump beams polarization and cell optical axis lie in the plane of incidence (xz plane), parallel to the grating vector $\mathbf{k} = k\mathbf{e}_x$. In the second one, s -polarized pump beams are used and the cell optical axis is oriented along \mathbf{e}_y , normal to \mathbf{k} (see Fig. 1). In both the arrangements the pump beams propagate as extraordinary waves.

In Fig. 2 we report the diffraction efficiency measurements versus the pump-beam intensity I_0 for both geometries, performed by means of a linearly polarized He-Ne laser probe-beam ($\lambda_p = 632.8$ nm). The optical modulation shows strong anisotropy in both cases; but while in the first one the p -polarized beam experiences the highest diffraction (η_p up to 30%) and the s -polarized beam is totally transmitted ($\eta_s \approx 0$) [see Fig. 2(a)], in the second one the p -polarized beam is totally transmitted ($\eta_p \approx 0$) and the s -polarized beam is highly diffracted (η_s up to 30%) [see Fig. 2(b)]. Diffraction efficiencies strongly depend on the probe-beam polarization, which are maxima for the extraordinary wave and

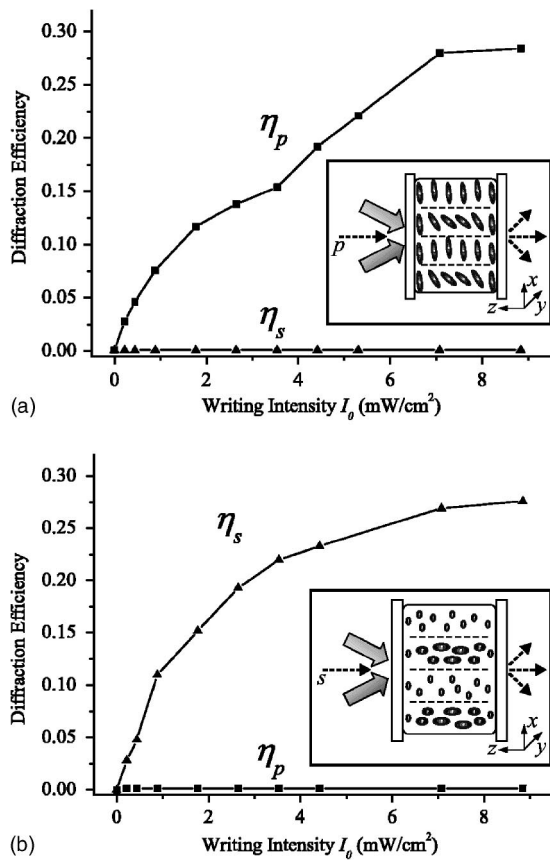


FIG. 2. The diffraction efficiency of the s - (▲) and p -polarized (■) He-Ne laser probe-beam is reported versus the writing beams intensity I_0 , for each investigated geometry. Only the p -polarized beam experiences diffraction when the cell optical axis is parallel to \mathbf{k} (a). Only the s -polarized beam is diffracted when the cell optical axis is normal to \mathbf{k} (b).

nearly zero for the ordinary wave, and they are comparable when beam polarization is parallel to the cell optical axis. This evidence implies that, in both geometries, only the extraordinary refractive index is spatially modulated along \mathbf{k} , and suggests that the optical gratings are due to spatial modulations of the nematic director which is restricted within the plane perpendicular to the cell surfaces and parallel to the rubbing direction, as sketched in the insets of Fig. 2.

It is worth noting that the gratings features do not depend on the polarization state of the pump beams, provided that light intensity modulation is present [16,17]; nevertheless self-diffraction (namely, diffraction of the pump beams) is maximum when the pump beams travel as extraordinary waves, because of the above described behavior. By choosing the pump-beam polarization parallel to the cell optical axis, we noted that in the first geometry [see Fig. 1(a)] the two p -polarized beams exhibit asymmetric energy transfer, that is an intensity increase for one beam and an equal decrease for the other when they simultaneously pass through the self-induced grating [16]. On the contrary, no energy transfer occurs for the two s -polarized beams in the second arrangement [see Fig. 1(b)], although self-diffraction is present in both cases. The asymmetric transfer of energy be-

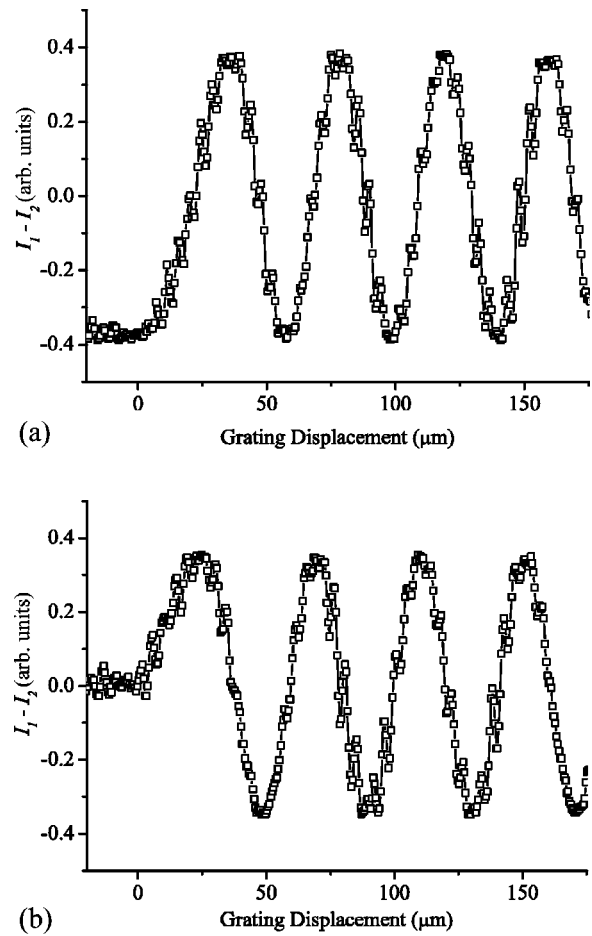


FIG. 3. The difference ($I_- = I_1 - I_2$) of the two transmitted pump beams intensities versus the cell displacement along \mathbf{k} is reported for the two investigated geometries. The initial phase of the signal I_- allows calculating the spatial phase shift of the grating: $\phi \approx \pi/2$ or $\phi \approx 0$ when the cell optical axis is parallel (a) or normal (b) to \mathbf{k} .

tween pump beams in self-diffraction configuration is strictly related to the presence of a spatial phase shift between the refractive index modulation and the intensity pattern [16], so that we expected a phase-shifted and an in-phase optical modulation, respectively, for the first and second geometries.

In order to give details of the optical modulation, TBC investigation by means of the grating's translation technique was performed, which allows one to determine the absorption coefficient and refractive index modulations amplitudes, as well as the spatial phase shifts of both amplitude and phase gratings [16,23]. The TBC experiment's results indicate that the gratings are mainly phase gratings, i.e., pure refractive index modulation, and give evidence of the local or nonlocal nonlinear optical response for the investigated geometries [21].

In Fig. 3 we report the difference between the transmitted beams intensities ($I_- = I_1 - I_2$) versus the grating displacement. The signals I_1 and I_2 were recorded after that the optical grating had reached the steady state [12], when the cell is translated along \mathbf{k} . The speed of the grating displacement is 500 $\mu\text{m/s}$, so that the acquisition time is less than the

characteristic times of the grating recording and relaxation (~ 10 s). Since pure phase gratings are induced, only the modulation in I_- is present, whereas the sum of the intensities ($I_+ = I_1 + I_2$) is constant versus the displacement and assumes the same value in the two geometries [21]. The two measurements were carried out in the same experimental conditions ($I_0 \approx 20 \mu\text{W}/\text{cm}^2$), except for the pump-beam polarizations and the cell optical axis orientation. Comparable refractive index modulation amplitudes $\Delta n \approx 9 \times 10^{-4}$ were calculated for the two geometries, whereas significantly different values were obtained for the spatial phase shifts $\phi \approx \pi/2$ in the first geometry [Fig. 3(a)] and $\phi \approx 0$ in the second one [Fig. 3(b)].

III. THEORETICAL APPROACH TO THE SIPRE

It is well accepted that the occurrence of energy transfer in self-diffraction configuration proves the optical modulation nonlocality and then the PR origin of the gratings [3,4]; but neither the reported diffraction anisotropy nor the in-phase or the $\pi/2$ phase-shifted modulation depending on the cell orientation are fully explicable via the standard PR effect. A conventional PR model states that photocharge generation and separation processes occur in the bulk due to the interference intensity pattern [$I(x) \propto 1 - \cos(kx)$], so that a volume charge density $\rho(x) \propto -\cos(kx)$ varies along the grating vector $\mathbf{k} = k\mathbf{e}_x$, but it is nearly uniform along the z axis. The space-charge electric field has a single $\pi/2$ phase-shifted modulated component along \mathbf{k} :

$$\mathbf{E}_{\text{PR}}(x) = -\mathbf{e}_x E_x \sin(kx). \quad (1)$$

Through the linear electro-optic effect, the internal electric field induces the refractive index grating, which is $\pi/2$ phase shifted with respect to the intensity pattern. The investigated effect differs from the conventional PR effect in that the relative phase shift changes from $\pi/2$ to zero by simply rotating the NLC cell's axis with respect to the grating vector, so that the induced grating changes from nonlocal to local. Moreover, according to earlier investigations [12,17–19], the observed PR-like effect, namely, the SIPRE, is due to a wavelength-dependent photomodulation of surface-charge density at the LC-polymer interface, instead of photoinduced charge generation and redistribution in the undoped NLC bulk. In the following, we discuss a simple charge distribution for the SIPRE and calculate the resulting space-charge electric field in the cell, which is suitable to account for the observed local and nonlocal behavior and the grating's anisotropy, through the dielectric NLC director re-orientation. Because of the surface-limited charge distribution, in fact, the resulting static electric field in the sample has a more complex expression than the conventional PR field in Eq. (1); in particular, we demonstrate that the electric field has two orthogonal modulated components, within the incidence xz plane.

A first approach to describe the space-charge electric field distribution in the NLC layer for the SIPRE is here performed in the Helmholtz double-layer charge distribution approximation [24], within the following limits. (a) NLC dielectric anisotropy is neglected, and a scalar dielectric

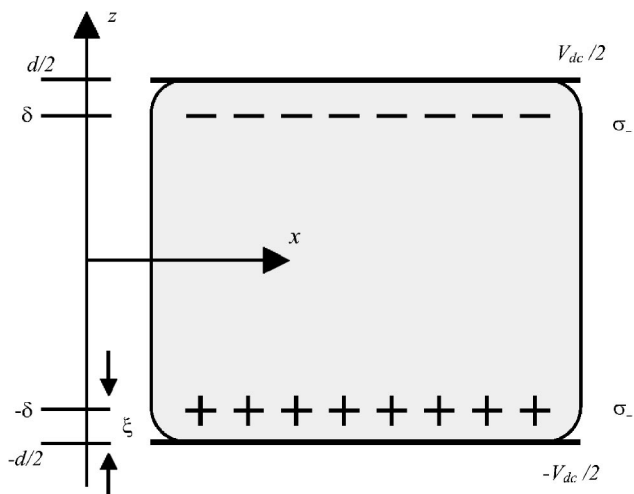


FIG. 4. Model scheme for charge distribution within the cell in the Helmholtz double-layer approximation.

constant $\epsilon = \epsilon_{\perp}$ is assumed [22]. (b) Ions are considered as dimensionless charges. (c) Selective ion adsorption at the polymer surfaces is disregarded (equal adsorption energy for anions and cations) [25]. (d) Ion diffusion current is negligible with respect to the conduction current.

We consider an internal NLC layer of thickness d , bounded by ion-blocking electrodes as sketched in Fig. 4. In thermodynamic equilibrium, commercial LCs contain a density n_0 of ions due to dissociated impurities contained in it. Without voltage between the electrodes, the ion volume density is uniform across the cell and equal for anions and cations $n_+(x, z) = n_-(x, z) = n_0$ and the layer is locally and globally neutral. When an external voltage V_{dc} is applied to the electrodes, the ions move along the z axis towards the electrode of opposite sign. In the limit of negligible diffusion current, the bulk density of ions is uniform across the NLC layer, except for two thin regions near the electrodes where charges are accumulated, whose thickness is comparable with the Debye screening length [24]. If the voltage is high enough, all the ions are drifted close to the electrodes and the NLC bulk remains free of ions. To model the charge distribution in the cell before the irradiation with the light intensity pattern, we fix the electrode potentials

$$V(z = d/2) = -V(z = -d/2) = V_{\text{dc}}/2 \quad (2)$$

and assume that ions are collected in two opposite charged layers, whose thickness is negligible with respect to d , and whose distance from the respective electrode is ξ . In the following,

$$\begin{aligned} \sigma_- &= \sigma(z = \delta) = -\sigma_0, \\ \sigma_+ &= \sigma(z = -\delta) = \sigma_0 \end{aligned} \quad (3)$$

are the anodic and the cathodic surface-charge densities, where $\delta = d/2 - \xi$ is the distance between each surface-charge layer and the cell's central plane $z=0$ (Fig. 4). Such an approximation allows us to analytically solve the Dirichlet problem for the electric potential $V(x, z)$ within the cell, by

means of the Laplace equation, exploiting the charge distribution symmetry, the boundary, and continuity (Gauss's and Faraday's laws) conditions.

The effective potential within the cell is described by a piecewise function restricted in the three charge-free regions

$$\begin{aligned} (a) \quad & \delta < z, \\ (b) \quad & -\delta < z < \delta, \quad \text{and} \\ (c) \quad & z < -\delta, \end{aligned} \quad (4)$$

where it is the sum of the σ_+ and σ_- related terms

$$V^i = V_+^i + V_-^i, \quad \text{for } i = a, b, c. \quad (5)$$

The Laplace equation for each V_+^i and V_-^i is solved reducing the partial differential equation to ordinary differential equations system, by the method of separation of variables [26,27]. The symmetry of the relative charge distribution allows the choice of the proper functional form for the solutions. The effective potential $V(z)$ in the regions (4) can be written as

$$V(z) = \begin{cases} V^a(z) = \left[\frac{2\sigma_0}{\epsilon d} \delta + \frac{V_{dc}}{d} \right] z - \frac{\sigma_0}{\epsilon} \delta, \\ V^b(z) = \left[\frac{V_{dc}}{d} - \frac{2\xi\sigma_0}{\epsilon d} \right] z, \\ V^c(z) = \left[\frac{2\sigma_0}{\epsilon d} \delta + \frac{V_{dc}}{d} \right] z + \frac{\sigma_0}{\epsilon} \delta. \end{cases} \quad (6)$$

Birefringence analysis, reported in Ref. [19], suggests that the voltage drop across the NLC bulk is nearly zero [$V^b(z) = 0$] only for $V_{dc} \leq 1.5$ V, then we consider that

$$\sigma_0 = \frac{\epsilon}{2\xi} V_{dc} \quad \text{for } V_{dc} \leq 1.5 \text{ V},$$

$$\sigma_0 = \sigma_0^{\text{sat}} \approx \frac{\epsilon}{2\xi} (1.5 \text{ V}) \quad \text{for } V_{dc} > 1.5 \text{ V}. \quad (7)$$

Preliminary experimental investigations on the PVA-E7 cells indicate that the thickness of the Helmholtz double layers at the interfaces is about 4 order of magnitude less than the cell gap, and so in the range of $10^{-3} \mu\text{m}$. Similar values have been reported in literature for cyanobiphenyls [28]. According to such values we can consider that ξ is comparable with the thickness of the PVA layers ($\xi \approx 10^{-2} \mu\text{m}$). The saturation value σ_0^{sat} allows us to estimate the volume density of the ions

$$n_0 = \frac{\sigma_0^{\text{sat}}}{qd} \approx 2 \times 10^{21} \text{ m}^{-3} \quad (8)$$

in which we assumed the ion charge $q = 1.6 \times 10^{-19}$ C and the dielectric constant $\epsilon = 5.2 \epsilon_0$ [29]. Previously published experimental results suggest that even the huge electric field ($\sim 10^3$ V/ μm) at the PVA-E7 interfaces does not significantly influence the anchoring conditions nor the director profile, which is instead perturbed by the electric field in the central cell region [19].

The first attempt to model the effective space-charge electric field when the cell is irradiated with an intensity pattern, are carried out assuming a linear dependence of the surface-charge density modulation on light intensity. Photocurrent and photoinduced birefringence studies [18,19] supported that light of proper wavelength produces surface-charge depletion at the anodic PVA-E7 interface only. This means that spatially modulated intensity pattern $I(x) = 2I_0[1 - \cos(kx)]$ results in a local modulation of the anodic charge density only:

$$\sigma_+ = \sigma_0, \quad \sigma_-(x) = -\sigma_0[1 + \cos(kx)]/2, \quad (9)$$

where we supposed a complete charge density depletion at the light intensity maxima [$x = (2m+1)\pi/k$ for $m \in \mathbb{Z}$]. The electrostatic potential is calculated through the Laplace equation, exploiting the charge distribution symmetry, the boundary and continuity conditions, as previously done for the uniform surface-charge densities (3). Due to the surface-charge density dependence on the x coordinate, the potential is now function of both x and z

$$V(x, z) = \begin{cases} \frac{\sigma_0 \xi}{4\epsilon} \left(1 - \frac{2z}{d} \right) \left(3 - \frac{d}{\xi} \right) + \frac{zV_{dc}}{d} + F(x, z) & \text{for } \delta < z, \\ \frac{\sigma_0 \xi}{4\epsilon} \left(1 - \frac{6z}{d} \right) + \frac{zV_{dc}}{d} - G(x, z) & \text{for } -\delta < z < \delta, \\ \frac{\sigma_0 \xi}{4\epsilon} \left(\frac{2d}{\xi} - 3 \right) \left(1 + \frac{2z}{d} \right) + \frac{zV_{dc}}{d} - G(x, z) & \text{for } z < -\delta, \end{cases} \quad (10)$$

where

$$F(x, z) = \frac{\sigma_0}{2\epsilon k} \frac{\sinh[k(d - \xi)] \sinh \left[k \left(z - \frac{d}{2} \right) \right] \cos(kx)}{\sinh(kd)},$$

$$G(x, z) = \frac{\sigma_0}{2\epsilon k} \frac{\sinh(k\xi) \sinh \left[k \left(z + \frac{d}{2} \right) \right] \cos(kx)}{\sinh(kd)} \quad (11)$$

and σ_0 satisfies Eq. (7). In Fig. 5 we report the $V(x, z)$ profile, which has been calculated for typical values of the physical parameters involved in the model. The graph shows the sinu-

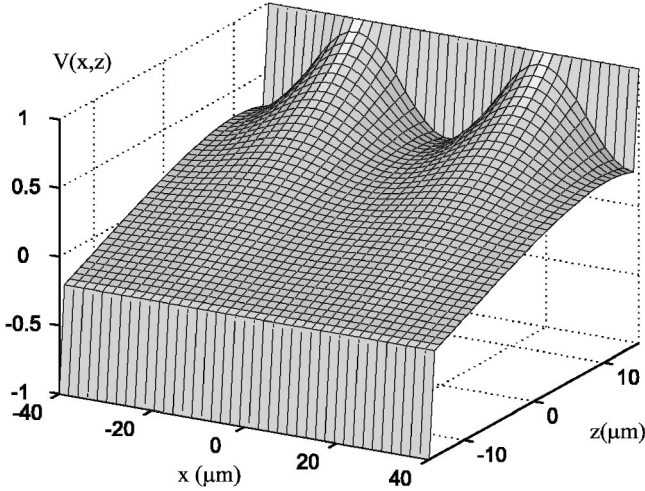


FIG. 5. The potential profile $V(x,z)$ within the cell has been calculated for the following values of the physical parameters $V_{dc} = 2.0$ V, $k = 2\pi/40$ μm^{-1} , $\xi = 10^{-2}$ μm , and $\epsilon = 5.2$ ϵ_0 .

soidal modulation of the potential as a function of x , mainly located near the anodic interface, whose amplitude decreases with decreasing z . The voltage drop at the anodic double layer and, consequently, the potential distribution along the z axis change along \mathbf{k} , due to the σ_- dependence on the x coordinate. The electric field components $E_x(x,z)$ and $E_z(x,z)$ within the LC bulk (for $-\delta < z < \delta$) has been calculated from Eqs. (10) and (11) by partial differentiations

$$E_x(x,z) = -A \sinh\left[k\left(z + \frac{d}{2}\right)\right] \sin(kx),$$

$$E_z(x,z) = -B + A \cosh\left[k\left(z + \frac{d}{2}\right)\right] \cos(kx), \quad (12)$$

where A and B include model's parameters, such as dielectric constant, double layer, and cell thicknesses:

$$A = \frac{\sigma_0 \sinh(k\xi)}{2\epsilon \sinh(kd)}, \quad B = \frac{V_{dc}}{d} - \frac{3\xi\sigma_0}{2\epsilon d}. \quad (13)$$

The model shows that electric field has two normal modulated components E_x and E_z . They are both spatially modulated along \mathbf{k} with the same periodicity of the interference fringes, but while E_x is $\pi/2$ phase shifted, E_z is in phase with respect to the intensity pattern $I(x)$.

IV. DISCUSSION AND CONCLUSIONS

The understanding of the local or nonlocal gratings, due to the SIPRE, needs to consider the dielectric interaction between the nematic director and the electric field distribution calculated above. The three-dimensional director structure can be determined through minimization of the Gibbs free-energy density (elastic and dielectric terms), taking into account the boundary conditions (i.e., infinite anchoring energy) [30]. Nevertheless, simple speculations about the grating diffraction anisotropy and the director configuration sym-

metry allow us to give reasons for the phases of the refractive index modulations in the investigated geometries.

The reported analysis of the diffraction efficiency proved that the director reorientation is always confined within the plane normal to the cell surfaces and parallel to the rubbing direction (insets of Fig. 2). In the second cell arrangement [Fig. 1(b)], this means that director is constrained in the yz plane and, subsequently, that the molecular reorientation is mainly induced by the E_z component. The E_x component would induce a twist deformation, yielding to a modulated director distortion out of the yz plane and then to nonzero diffraction for the p -polarized light. The E_x contribution to the director distortion can be neglected because the p -polarized beam does not show significant diffraction ($\eta_p \approx 0$). The dielectric free-energy term depends quadratically on the electric field, but because E_z is sum of a uniform and a spatially modulated component [see Eq. (12)] the director distortion has the same periodicity (Λ) and the same phase of E_z . The refractive index grating is, then, in phase with the interference pattern ($\phi = 0$).

In the first arrangement [Fig. 1(a)], the director is confined in the xz plane, and both E_x and E_z components contribute to the director configuration. The actual $\pi/2$ phase shift of the refractive index grating can be explained simply considering the dielectric torque Γ_E caused by the interaction between the electric field in Eq. (12) and the director \mathbf{n} :

$$\Gamma_E = \Delta\epsilon(\mathbf{n} \cdot \mathbf{E})(\mathbf{n} \times \mathbf{E})$$

$$\approx -\mathbf{e}_y \Delta\epsilon \times \sin(2\theta) \left\{ \frac{B^2}{2} - AB \cosh\left[k\left(z + \frac{d}{2}\right)\right] \cos(kx) \right\}$$

$$+ \mathbf{e}_y \Delta\epsilon \cos(2\theta) AB \sinh\left[k\left(z + \frac{d}{2}\right)\right] \sin(kx), \quad (14)$$

where θ is a homogeneous reorientation angle of \mathbf{n} , which is comparable with the pretilt angle. The competition between dielectric and elastic torque results in the periodic director field modulation along \mathbf{e}_x . In Eq. (14) we have neglected the terms which depend on A^2 since, taking into account the estimated values of the model's parameters in Eq. (13), we calculated $B \approx 60A$. In the limit of small θ , i.e., for effective voltage drop across the NLC bulk near to the Fredericksz threshold [see Eq. (6)], Eq. (14) can be written as

$$\Gamma_E \approx -\mathbf{e}_y \Delta\epsilon \left\{ \sin(2\theta) \frac{B^2}{2} \right.$$

$$\left. - \cos(2\theta) AB \sinh\left[k\left(z + \frac{d}{2}\right)\right] \sin(kx) \right\}. \quad (15)$$

To the first order approximation, Γ_E shows a spatially modulated term along \mathbf{e}_x which has the same periodicity and phase of the E_x field component [see Eq. (12)]. Therefore, the resulting director and refractive index modulations should be $\pi/2$ phase shifted with respect to the interference pattern, as experimentally reported.

In conclusion, we report a simple model for surface induced photorefractive effect that supports the results of FLS and TBC experiments well. In contrast to the conventional

PR effect, the measurements show that in-phase or $\pi/2$ phase-shifted refractive index modulation can be obtained in the same experimental conditions, provided that the cell optical axis is normal or parallel with respect to the grating vector. The main difference between the conventional and surface induced PR effect is the charge distribution within the sample: in the former case a charge density modulation in the bulk is considered, in the second case a modulated

surface-charge distribution near the interface is assumed. A first charge distribution model for the SIPRE has been discussed. Due to light-induced modulation of the anodic surface-charge density, the resulting electric field exhibits two modulated components, one is parallel to the grating vector ($\pi/2$ phase shifted) and the other is orthogonal to the cell's surfaces (in phase). The electric field within the NLC cell accounts for the reported experimental observations.

-
- [1] P. Gunter and J.-P. Huignard, *Photorefractive Materials and Their Applications* (Springer-Verlag, Berlin, 1989), Vols. I and II.
- [2] P. Yeh, *Introduction to Photorefractive Nonlinear Optics* (Wiley, New York, 1993).
- [3] W. E. Moerner, A. G. Jepsen, and C. L. Thompson, *Annu. Rev. Mater. Sci.* **27**, 585 (1997), and references therein.
- [4] G. P. Wiederrecht, *Annu. Rev. Mater. Res.* **31**, 139 (2001), and references therein.
- [5] K. Sutter and P. Gunter, *J. Opt. Soc. Am. B* **7**, 2274 (1990).
- [6] S. Ducharme, J. C. Scott, R. J. Twieg, and W. E. Moerner, *Phys. Rev. Lett.* **66**, 1846 (1991).
- [7] E. V. Rudenko and A. V. Sukhov, *JETP* **78**, 875 (1994), and reference therein.
- [8] H. Ono and N. Kawatsuki, *Appl. Phys. Lett.* **71**, 1162 (1997).
- [9] F. Simoni, G. Cipparrone, A. Mazzulla, and P. Pagliusi, *Chem. Phys.* **245**, 429 (1999), and references therein.
- [10] G. P. Wiederrecht, B. A. Yoon, and M. R. Wasielewski, *Adv. Mater. (Weinheim, Ger.)* **12**, 1533 (2000).
- [11] I. C. Khoo, M. Y. Shih, A. Shishido, P. H. Chen, and M. V. Wood, *Opt. Mater. (Amsterdam, Neth.)* **18**, 85 (2001), and references therein.
- [12] P. Pagliusi and G. Cipparrone, *Appl. Phys. Lett.* **80**, 168 (2002).
- [13] I. C. Khoo, J. Ding, Y. Zhang, K. Chen, and A. Diaz, *Appl. Phys. Lett.* **82**, 3587 (2003).
- [14] A. Golemme, B. Kippelen, and N. Peyghambarian, *Chem. Phys. Lett.* **319**, 655 (2000).
- [15] J. Zhang, V. Ostroverkhov, K. D. Singer, V. Reshetnyak, and Y. Reznikov, *Opt. Lett.* **25**, 414 (2000).
- [16] P. Pagliusi, R. Macdonald, S. Bush, G. Cipparrone, and M. Kreuzer, *J. Opt. Soc. Am. B* **18**, 1632 (2001).
- [17] P. Pagliusi and G. Cipparrone, *J. Opt. Soc. Am. B.* (to be published).
- [18] P. Pagliusi and G. Cipparrone, *J. Appl. Phys.* **92**, 4863 (2002).
- [19] P. Pagliusi and G. Cipparrone, *J. Appl. Phys.* **93**, 9116 (2003).
- [20] V. Boichuk, S. Kucheev, J. Parka, V. Reshetnyak, Y. Reznikov, I. Shiyonovskaya, K. D. Singer, and S. Slussarenko, *J. Appl. Phys.* **90**, 5963 (2001).
- [21] P. Pagliusi and G. Cipparrone, *Opt. Lett.* **28**, 2369 (2003).
- [22] G. Zhang, G. Montemezzani, and P. Gunter, *J. Appl. Phys.* **88**, 1709 (2000).
- [23] V. Kondilenko, V. Markov, S. Odulov, and M. Soskin, *Opt. Acta* **26**, 239 (1979).
- [24] J. N. Israelachvili, *Intermolecular and Surface Forces*, 2nd ed. (Academic Press, London, 1992).
- [25] D. Olivero, L. R. Evangelista, and G. Barbero, *Phys. Rev. E* **65**, 031721 (2002).
- [26] J. Irving and N. Mullineux, *Mathematics in Physics and Engineering* (Academic Press, New York, 1959), Vol. 6, Chap. 1.
- [27] K. F. Riley, *Mathematical Methods for the Physical Sciences* (Cambridge University Press, London, 1974), Chap. 10.
- [28] S. Murakami and H. Naito, *Jpn. J. Appl. Phys., Part 1* **36**, 773 (1997).
- [29] R. N. Thurston, J. Cheng, R. B. Mayer, and G. D. Boyd, *J. Appl. Phys.* **56**, 263 (1984).
- [30] P. G. de Gennes and J. Prost, *The Physics of Liquid Crystals*, 2nd ed. (Clarendon Press, Oxford, 1996), Chap. 3.